Die Küste, 72 (2007), 105-123

Propagation of a Tsunami-Wave in the North Sea

By Rainer Lehfeldt, Peter Milbradt, Andreas Plüss and Holger Schüttrumpf

Zusammenfassung

Die Tsunami-Katastrophe in Asien am 26. Dezember 2004 war der Anlass, das Risiko für einen Tsunami in der Nordsee und die Auswirkungen für die deutsche Küste zu untersuchen. Dazu wurden im Januar 2005 numerische Simulationen durchgeführt, um die Ausbreitung einer Tsunami-Welle in der Nordsee zu studieren und die besonders betroffenen Küstenabschnitte zu identifizieren. Veranlassung waren eine Reihe von Anfragen an die Autoren hinsichtlich des Gefährdungspotentials in der Nordsee. Der vorliegende Beitrag wurde auf der Grundlage dieser Simulationen erstellt. Es konnte gezeigt werden, dass die Deutsche Bucht durch die geringe Wassertiefe des Wattenmeeres gut geschützt ist. Dies ist nicht der Fall für die niederländische Küste und die Britischen Inseln, die erheblich stärker betroffen sein würden. Ein Tsunami, der durch den Ärmelkanal einlaufen würde, hätte keine wesentlichen Auswirkungen in der Nordsee, da diese Welle bereits im Ärmelkanal reflektiert und gedämpft würde.

Summary

The tsunami disaster in Asia on December 26, 2004, was a reason to reconsider the risk of a tsunami in the North Sea and the risk of a tsunami impact on the German coast. Therefore, numerical simulations were performed in January 2005 in order to study the propagation of a tsunami wave in the North Sea and to find out the most affected areas in the North Sea and in the German Bight. Motivation for this work were questions put to the authors concerning the risk potential in the North Sea. This paper sums up the findings of numerous simulations. It could be shown that the German Bight is well protected against a tsunami wave by the shallow water of the wadden sea. This is not the case for the Dutch coast and the British Isles which would be significantly affected by a tsunami. A tsunami entering the North Sea through the English Channel will not have any severe consequences in the North Sea, since this wave will be reflected and dampened in the English Channel.

Keywords

North Sea, German Bight, tsunami risk, tsunami modeling, shallow water waves, multi model simulation, wave propagation.

Contents

1. Introduction and Motivation

The earthquake of December 26, 2004, in the vicinity of the island of Sumatra and the resulting tsunami wave caused one of the major natural disasters of the last centuries. The majority of tsunamis are generated by seaquakes, but tsunamis can also be generated by volcano eruptions or flank failures due to slope instabilities for which the eruption of the Krakatau in 1883 and the Storegga-sliding about 6000 B.C. are prominent examples. The probability of sea quakes is lower in the Atlantic Ocean than in the Asian region due to the continental drift. Nevertheless, disastrous tsunamis have also occurred in the Atlantic Ocean. An example is the destruction of Lisbon in 1755 by a tsunami wave.

Thus, the generation of a tsunami in the Atlantic Ocean and its propagation into the North Sea is possible. However, no data is available concerning the propagation of a tsunami wave in the shallow North Sea and its impact on the coastlines and estuaries. Hence, the objective of the present study is the propagation of a tsunami wave in the North Sea. The probability of occurrence and the cause for a tsunami were not investigated.

Different hydrodynamic numerical models were applied to study this phenomenon. The input wave at the seaward boundary was calculated analytically both from the solitary wave theory and an approximation by long waves. The propagation of the waves was investigated for three different scenarios:

- without tidal influence,
- including tidal influence,
- under storm surge conditions.

After that, the different scenarios were compared, and the impact of a tsunami on the German coast was determined from the maximum wave height. In addition, areas of high morphodynamic strain can be identified from an evaluation of maximum velocities.

Finally, some conclusions for future research are drawn.

2. Tsunami Wave Theory

Tsunamis generated by seaquakes are long periodic waves ranging between wind and tidal waves (Fig. 1). A tsunami wave can have a wavelength L exceeding 100 km and a wave period in the order of one hour in “deep water”. Because of its length, a tsunami is always a shallow-water wave, which is characterized by a very small ratio between the water depth and its wave length ($d/L < 0.05$). Shallow-water waves move with a celerity

$$c = \sqrt{g \cdot d}$$

with g = acceleration of gravity, d = water depth.

In the North Sea with a mean water depth of about 90 m the ratio between the water depth and the wave length for a tsunami wave is about d/L = 0.001 under the assumption of L = 100 km.

In free surface flow within relatively thin layers, the horizontal velocities are of primary importance, and the problem can be reasonably approximated by a quasi 2-dimensional system. The resulting equations, called shallow-water equations, include a term for the free-surface elevation H in addition to the horizontal velocities and can be written in the same conservational form as the 2D Euler equations for isothermal compressible flow where the water depth is equivalent to the gas density in Euler equations. Therefore, experience obtained from 2D Euler flow can be applied to the simulation of tsunamis:

- Singular impulsive disturbance which displaces the water column.
- Vertical displacement which is normally caused by seismic events, underwater landslides or a combination of the two.

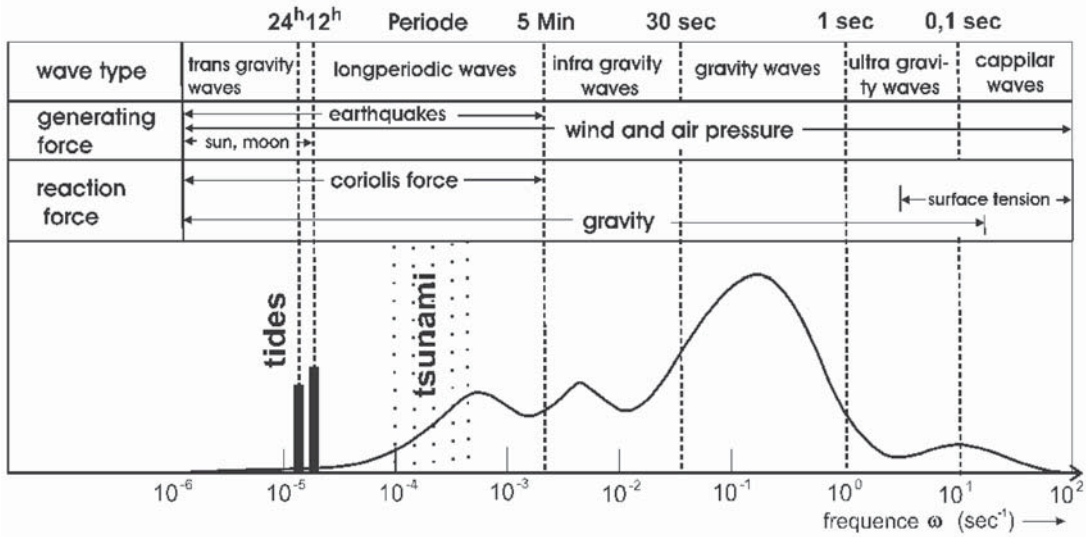

Fig. 1: Classification of surface waves according to the amplitude spectrum, after DIETRICH et al. (1975)

Using the Ursell parameter as a means to determine the importance of nonlinearities

$$U_r = \frac{(H/L)}{(d/L)^3}$$

we conclude based on the ratios H/L <<1 and d/L << 1 that nonlinear effects can be neglected in large parts of the Atlantic ocean.

Assuming a tsunami wave entering from the Atlantic Ocean with an amplitude of H = 1 m at the Northern entrance (d ≈ 300 m) and a wavelength L ≈ 100 km, the Ursell parameter is in the order of U_r = 400. This means, that the influence of the nonlinearities is increasing.

A Tsunami wave travelling across the North Sea towards the shoreline is transformed mainly by shoaling, refraction and reflection. In this region, nonlinearities cannot be neg-

lected anymore, and the fully nonlinear shallow water equations must be applied to solve the problem. The Ursell-Parameter increases rapidly in shallow waters reaching about Ur ≈ 10^7 in 10 m water depth. Thus, the importance of considering nonlinearities in the governing equations is demonstrated.

Wave shoaling causes a significant increase of wave heights in very shallow water. Another cause for locally increasing wave heights is the bay effect, which explains why severe damage occurred predominantly in bays during previous tsunamis. Both effects are described below.

2.1 Shoaling

Fig. 2 shows the shoaling effect according to linear wave theory. Even though linear theory is not valid in this region the main processes can be approximated by it. Wave shoaling follows a relationship $H \sim 1/d_x^{1/4}$ where d_x is the water depth in the onshore direction. In addition, the wave length is decreasing resulting in a steeper wave. Thus, shoaling is an important effect to be considered.

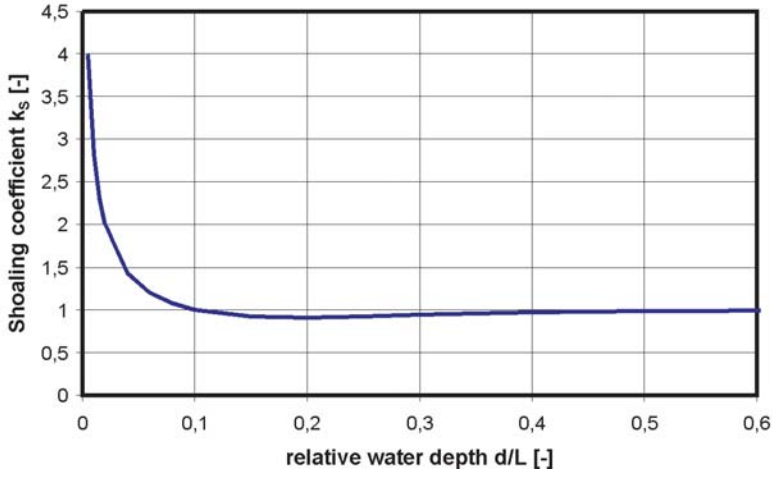

Fig. 2: Shoaling (according to Linear Wave Theory)

2.2 Bay effect

The wave height at position x is increasing with decreasing bay width and water depth. The bay effect can be calculated by Green's law (1837), which assumes no energy losses, no reflection and small wave heights:

$$\frac{H_x}{H_0} = \sqrt[2]{\frac{b_0}{b_x}} \sqrt[4]{\frac{d_0}{d_x}}$$

with: H = wave height, b = bay width, d = water depth, index 0 = offshore, x = onshore.

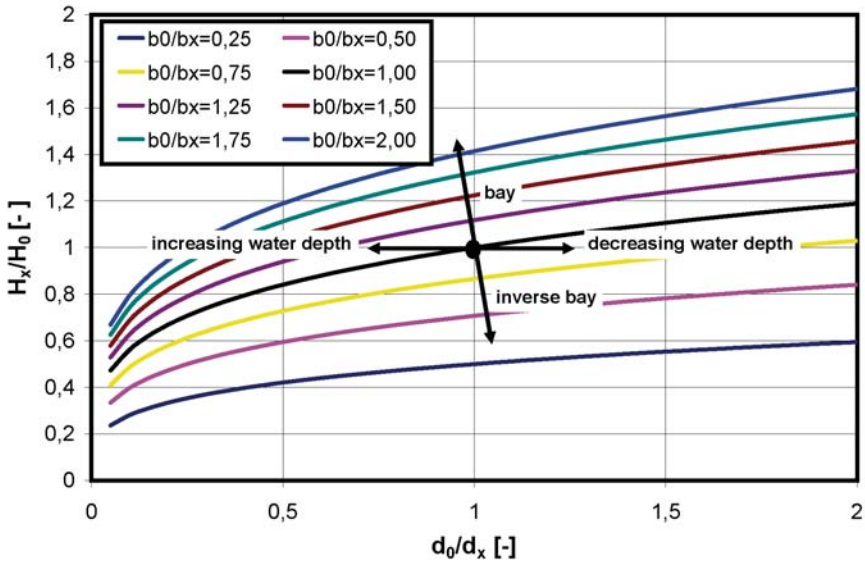

Fig. 3: Bay effect calculated by Green's law

Fig. 3 shows the dependency of the relative wave height (H_x/H_0) on the relative bay width b_0/b_x and the relative water depth d_0/d_x. Thus, it can be concluded that the wave evolution follows the laws $H_x \sim 1/d_x^{1/4}$ and $H_x \sim 1/b_x^{1/2}$. This was confirmed experimentally by SYNOLAKIS and SKJELBREIA (1993) for solitary waves using various laboratory data.

In addition to the processes described above, the tsunami wave is transformed by wave refraction, wave diffraction, wave breaking and energy losses due to bottom friction and wave breaking. These processes will not be discussed in detail in the present study.

2.3 Wave Run-up

Finally, a solitary wave hits the shoreline and can flood the hinterland thereby causing disaster. Several attempts were made to describe the run-up process by using Boussinesq-equations (STRYBNY, 2004) or the nonlinear shallow-water equations (CARRIER and GREENSPAN, 1958; TUCK and HWANG, 1972; SPIELVOGEL, 1976; SYNOLAKIS, 1987). Engineering equations to describe the run-up process were derived by SYNOLAKIS (1987) and LI and RAICHLEN (2001) for solitary waves:

$$\frac{R}{h_0} = 2{,}831\sqrt{\cot\beta}\left(\frac{H}{h_0}\right)^{5/4} + 0{,}104\cot\beta\,\frac{H}{h_0}$$

where H = solitary wave height, h_0 = water depth at the toe of the slope and β = slope. R is the wave run-up height, defined as the vertical distance between SWL and the highest point of wave run-up.

Numerical calculations of wave run-up and wave run-down for solitary waves were performed by LIN et al. (1999) by using a RANS-model and by STRYBNY (2004) by using a Boussinesq-model. These processes can also be approximated by hydrodynamic numerical

simulation models based on the shallow water equations with sophisticated flooding and drying algorithms.

Flooding of the hinterland by tsunami-waves is similar to wave run-up for non-breaking waves on smooth slopes. The up-rushing water is travelling far inland with high run-up velocities and therefore high wave run-up levels. In addition, high velocities also occur during wave run-down. These are reasons for the disastrous effects of tsunami waves.

3. Model Set-up and Boundary Control

3.1 Model Area and Model Grid

The set-up of a hydrodynamic numerical (HN)-model of the North Sea and the German Bight including the German estuaries first described by PLÜSS (2003) requires a

- substantial extent of the modeling domain,
- relatively high resolution of the bathymetry data within the coastal area and the estuaries and, consequently,
- large number of nodal points.

The high flexibility and variability of the computational grid needed for this integrated modeling approach can only be realized by an unstructured triangular grid topology.

The domain of the North Sea model covers the entire area between Scotland/England and Norway/Denmark/Germany in West/East direction and North/South between a line near

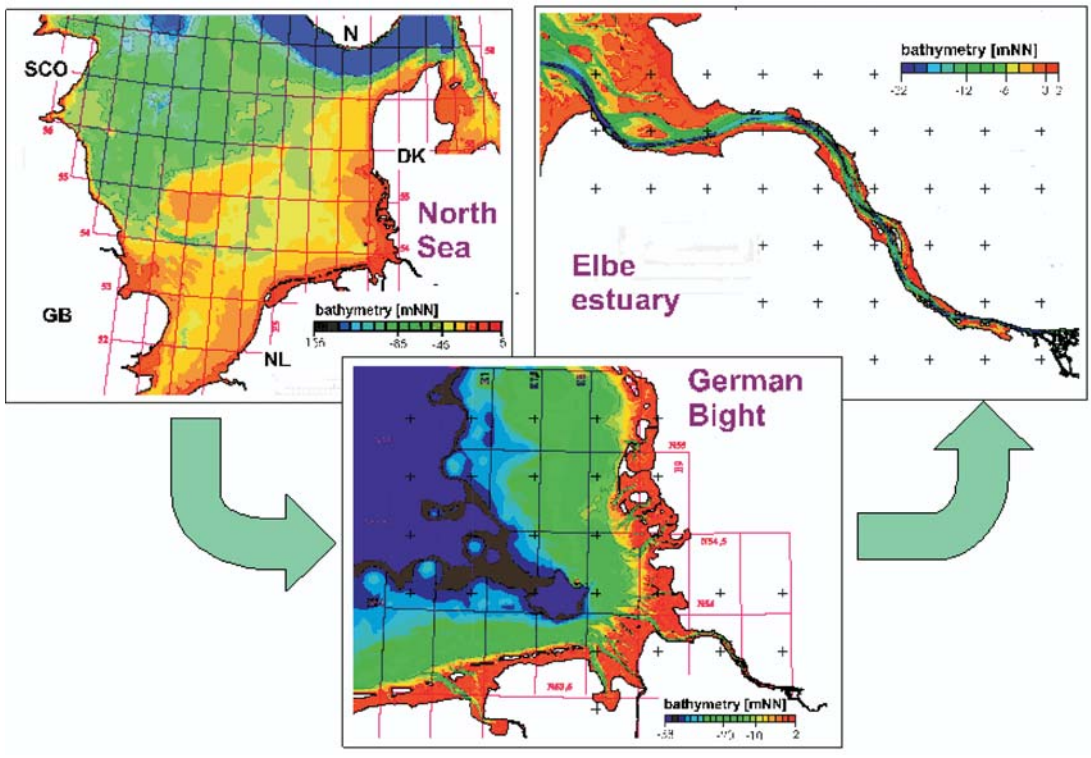

Fig. 4: The model area of the North Sea and detailed bathymetry reproductions in the German Bight and the Elbe estuary

Fair Island/Stavanger and Plymouth/Ile de Batz in the English Channel. The bathymetry data used here were was provided by the British Oceanographic Data Centre (BODC) and various German authorities responsible for the German Bight and the German estuaries.

In its present state, the model has 111,000 nodes with a grid spacing between 14 km in the outer North Sea and about 200 to 600 m in the German Bight (for details refer to: http://www.baw.de/vip/abteilungen/wbk/Publikationen/fachz/NSEE_Modell_BAWDH.pdf). The extent of the model area and the bathymetry are shown in Fig. 4 with detailed views of the German Bight and the Elbe estuary.

All scenarios with long waves are carried out in this domain with identical computational grids. The computational grid must resolve the input signal adequately, i.e. by at least 5 to 7 nodes per wave length. This condition is easily met by the existing tidal model with maximum grid size of 14 km in the boundary region.

In order to approximate a tsunami wave according to the solitary wave theory illustrated in Fig. 5, the grid spacing was refined. By assuming a wave length of about 15 km in deep water (d = 300 m) a grid resolution of about 3 km is necessary at the Northern entrance of the North Sea.

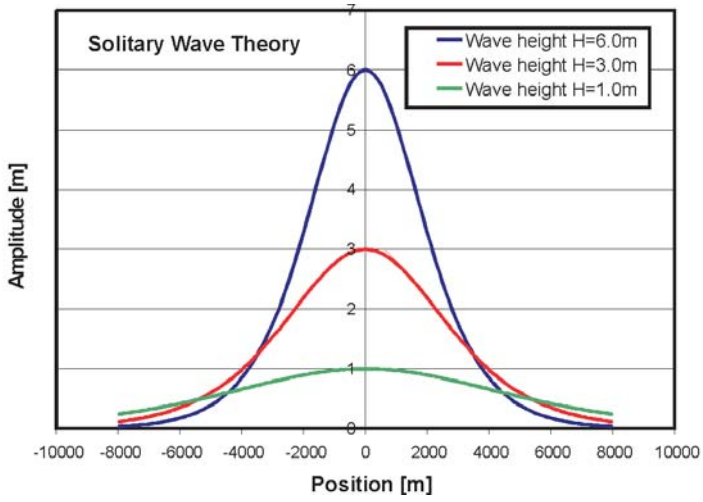

Fig. 5: Wave length of a solitary wave for d = 300 m

By refining the existing model a high-resolution grid with about 485,000 nodes and grid sizes ranging from maximum node spacing of 2.5 km at the Northern entrance to 10 m in coastal waters was created.

Fig. 6 shows the four main features which characterize the bathymetry of the North Sea. The Norwegian Trench with a depth of d ⩾ 200 m, two shallow areas, i.e. the Ling Bank at the Northern entrance and the Doggerbank with d = 30 m in the South West, which are surrounded by rather uniform water depths of d = 100 m and the wide shallow waters along the Dutch, German and Danish coasts. These features are clearly reflected in the propagation of all tsunami scenarios discussed below.

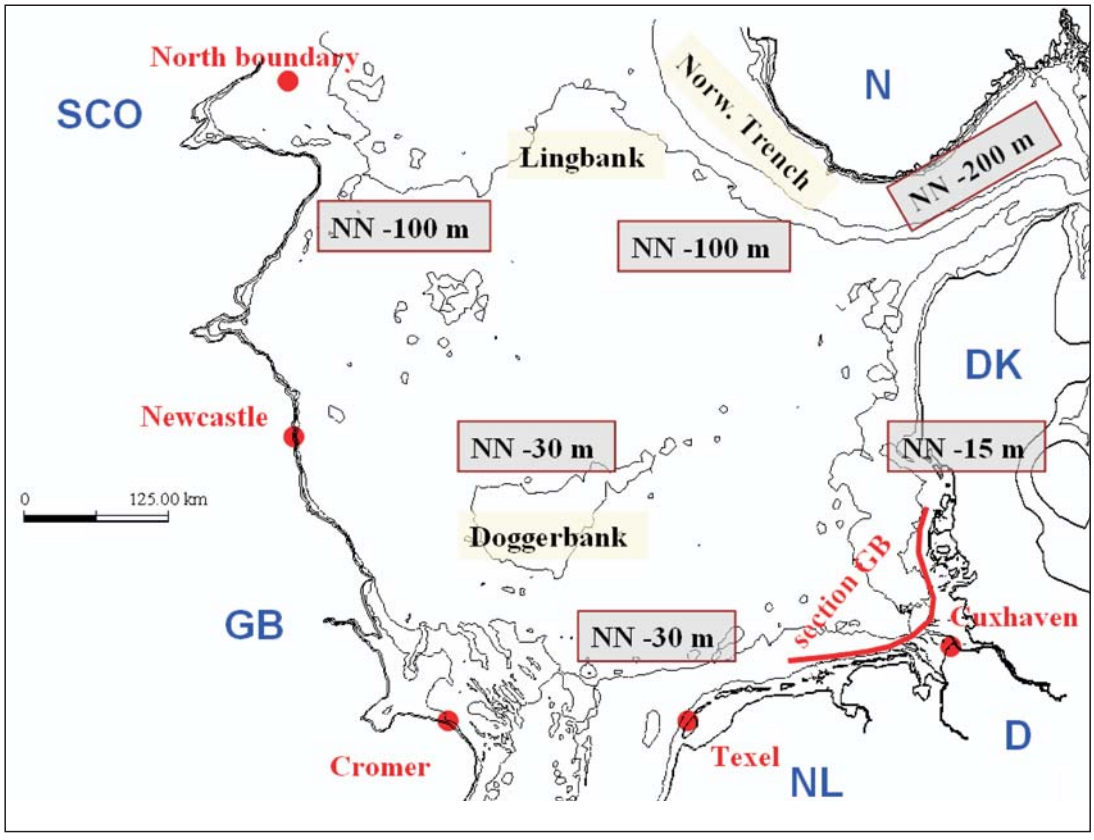

Fig. 6: Bathymetry features of the North Sea

3.2 Boundary Control

Since the propagation of a fictitious tsunami was investigated variations of wave height and wave shape were simulated. So-called "long geometrical waves" as well as solitary waves (see Fig. 7) with a given height and period were generated as boundary conditions. The solitary wave was calculated for an average water depth of d = 300 m according to the formulations by DEAN and DALRYMPLE (1991) based on the shallow water wave theory developed by KORTEWEG and DEVRIES in 1895:

$$\eta = H \sec h^2\left(\sqrt{\frac{3 \cdot H}{4 \cdot d^3}} \cdot c \cdot t\right)$$

with η = surface elevation, H = wave height, d = water depth,
t = time, c = wave celerity = $\sqrt{g\,(H + d)}$

The amplitudes of the boundary waves are chosen in the range of the measured amplitudes of the Sumatra tsunami as shown in Fig. 8 and Fig. 9. The tidal elevations of the Sumatra tsunami were determined from satellite data (NOAA) about 2 hours after the seaquake. The tidal elevations in the Indian Ocean were <1 m (Fig. 8). It has to be mentioned, however, that

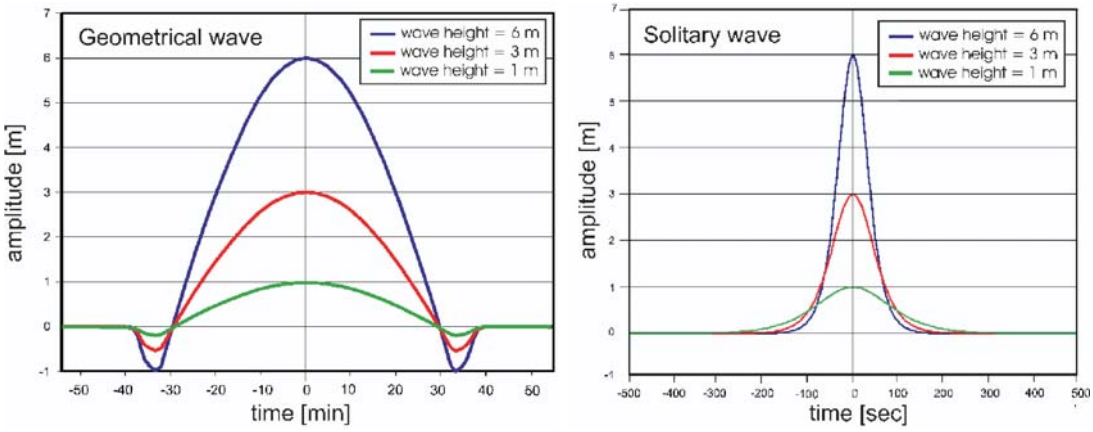

Fig. 7: Long geometrical waves in comparison to solitary wave

wave heights of the Sumatra tsunami measured nearshore, i.e. including the shoaling effect, were more than 1 m. Thus, a wave height in between 1 m and 2 m appears to be a realistic estimate on the continental shelf while higher waves are likely to occur nearshore.

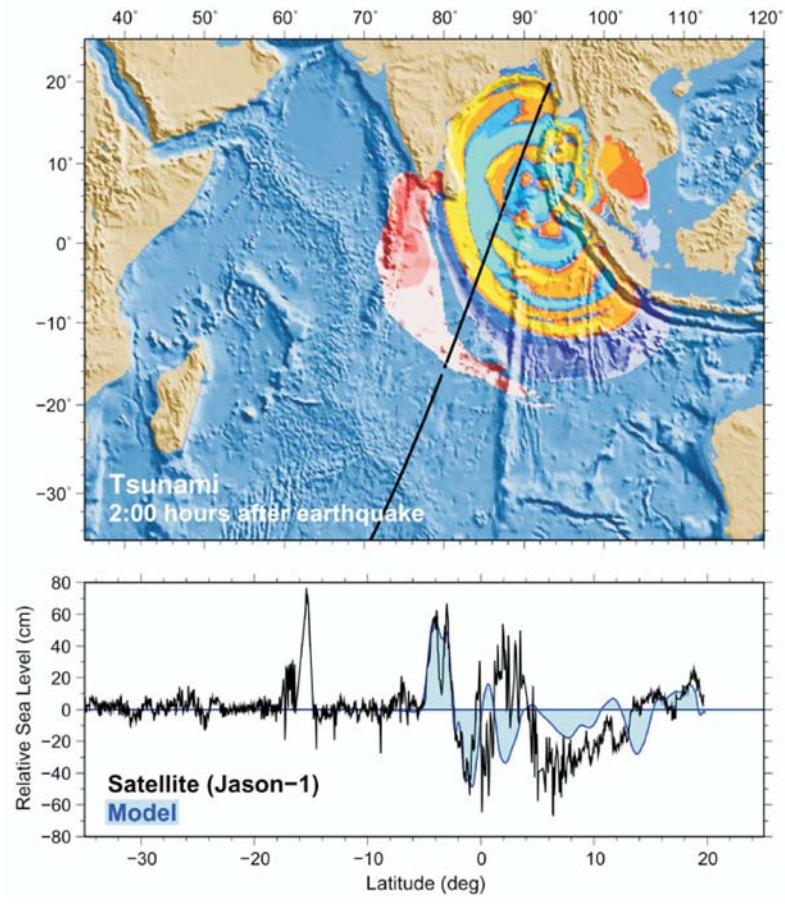

Fig. 8: Satellite data from Sumatra Tsunami (NOAA Magazine, 2005)

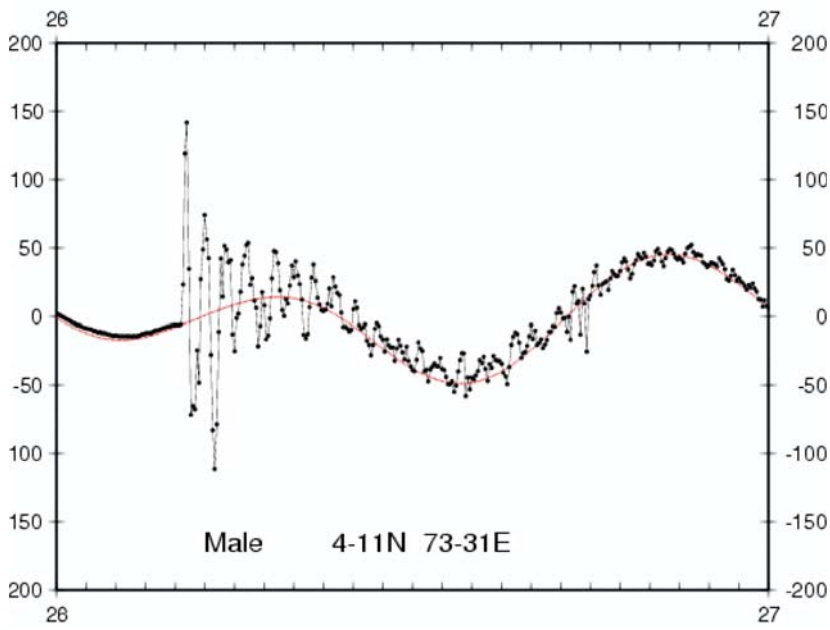

Fig. 9: Water level measurements at Male, December 26, 2004
(DEPARTMENT OF METEOROLOGY, MALDIVES, 2004)

Therefore, boundary wave heights were varied between H = 1 m and H = 6 m, which is assumed to be a realistic range. The periods of the fictitious tsunami in the North Sea are in good agreement with the observed periods of the Sumatra tsunami (Fig. 9) which were in the order of 15 to 20 min at Male (Maldives).

In addition, a tsunami entering the English Channel was also generated. The results showed that the water level elevations in the German Bight are not significantly influenced by this tsunami because of wave damping and wave reflection in the channel. Hence, this scenario is not presented here.

3.3 Short Description of Applied Numerical Models

Motivation for the multi model simulation was to study the propagation of tsunami waves in the relatively shallow North Sea and to estimate the effects related to their entering the German estuaries. Applicable numerical models have to represent shallow water effects and must handle the flooding and drying processes satisfactorily (PLÜSS and SCHÜTTRUMPF, 2004).

The chosen simulation models Untrim (CASULLI and WALTERS, 2000), Martin (MILBRADT, 2000) and Telemac (HERVOUET, 2007) are using unstructured grids for discretizing the bathymetry with variable grid resolution according to the bathymetric structures to be covered. The grid topology outlined in section 3.1 is identical for all three numerical schemes. However, the water depth is taken at the location of the grid nodes in Martin and Telemac, while it is taken at the center of the grid edges in Untrim.

Untrim can be run in hydrostatic and non-hydrostatic modes for comparison of 2d and 3d simulations. There was little difference in the resulting water levels and velocities for the selected test cases and no further details will be given here.

3.3.1 Untrim

Untrim is a Finite Element/Finite Volume model which solves the 2D/3D Reynolds-averaged Navier Stokes (RANS) equations for an unstructured orthogonal grid. Untrim was developed by CASULLI and WALTERS (2000) with a validation document provided at http://www.baw.de.

Untrim models the following processes within a water body:

- Propagation of long and short waves at the free surface,
- advective transport,
- horizontal and vertical turbulent diffusion,
- hydrostatic and non-hydrostatic pressures,
- Coriolis acceleration,
- horizontal and vertical gradients of density and
- bottom and wind friction.

Thus, Untrim can be applied to the present problem. In addition, Untrim can be used for transport calculations (sediment, heat, salt), which was not required for the present study.

3.3.2 Martin

The Martin simulation system is a powerful integrated public domain modeling tool for free-surface flows. Martin-Current2d is used to simulate free-surface flows in two dimensions of horizontal space. At each point of the mesh, the program calculates the water elevation and the two velocity components.

Martin-Current2d takes into account the following phenomena:

- Propagation of long waves, taking into account non-linear effects,
- bed friction,
- influence of Coriolis force,
- influence of meteorological factors: atmospheric pressure and wind,
- turbulence,
- influence of horizontal temperature or salinity gradients on density and
- dry areas in the computational domain: intertidal flats and flood plains.

Martin-Current2d solves the transient shallow water equations using a high-precision stabilized finite-element method on an unstructured grid of triangular elements. The controlling of the internal time steps takes place automatically and as a function of the selected time integration schema. The implemented strategy for flooding and drying is highly volume conserving.

The model is implemented in AnsiC and a paralleled version of the software is also available based on OpenMP. A detailed description of the code is available online (MILBRADT, 2000).

3.3.3 Telemac

The mathematical model Telemac-2D is based on the finite element approach. Telemac-2D was designed to solve several depth-integrated transient non-linear partial differential equations. The model is actually used to study one or more of the following physical processes:

- Transport of water (conservation of the water mass),

- transport of linear momentum (conservation of linear momentum),
- transport of turbulent kinetic energy and turbulent kinetic energy dissipation (conservation of the turbulent kinetic energy) and
- transport of salinity (conservation of the dissolved salt mass).

Telemac-2D was developed by Laboratoire Nationale d'Hydraulique of Electricté de France, Direction des Etudes et Recherches (EDF-DER), Chatou-Paris. A detailed description of the code (HERVOUET, 2007) is available at http://www.baw.de/vip/en/ departments/ department_k /methods/hnm/mac2d/mac2d-en.html.

4. Model Results

The models used differ considerably with respect to numerical schemes and physical approximations and simplifications, respectively, which are in turn reflected in the simulation results. Intercomparison of these results shows, that such model effects introduce an uncertainty which defines a range of validity for results of different input scenarios. For the tsunami scenarios we conclude that the three models perform in a very similar way.

4.1 Tsunami Propagation without Tidal Influence

The propagation of an incoming tsunami at the Northern boundary of the North Sea between Wick (Scotland) and Stavanger (Norway) with a height of about 6 m (time t = 4.0 h) was investigated (Fig. 10) using the geometric wave input signal.

The wave celerity $c = \sqrt{g \cdot d}$ in the Norwegian Trench with water depths of more than 200 meters is much higher than in the central part of the North Sea with water depths between d = 100 to 120 m. This results in a spreading of the incoming tsunami including a decrease of the wave height (time t = 5.5 to 7.0 h).

Now, the wave is propagating along the Danish coast towards the German Bight. The first tsunami wave hits the German coast about 7 hours after arrival in the North Sea (time t = 11.5 to 13.0 h).

Shallow water regions such as the Ling Bank (d = 60 to 70 m) or the Doggerbank (d = 20 to 30 m) cause refractions and an increase of the wave height. The resulting wave enters the Northern entrance of the English Channel.

The tsunami wave hitting the English coast is partially reflected and propagates as a second wave from West to East. This second wave enters the German Bight between times t = 8.5 to 14.5 h.

The reflection effect can be clearly seen at time 8.5 h east of the Firth of Forth. At this time, the second wave train is generated and travels towards the German Bight. In addition, the bay effect is obvious in the Firth of Forth at the same time.

Finally, wave disturbances generated by reflection effects in the entire North Sea can be observed (Fig. 10). At 14.5 hours after arrival at the Northern entrance two regions in the Southern North Sea are considerably affected. Wave heights of about 1.5 m appear at the Northern Dutch coast along the West Frisian Islands and at the Dutch West coast.

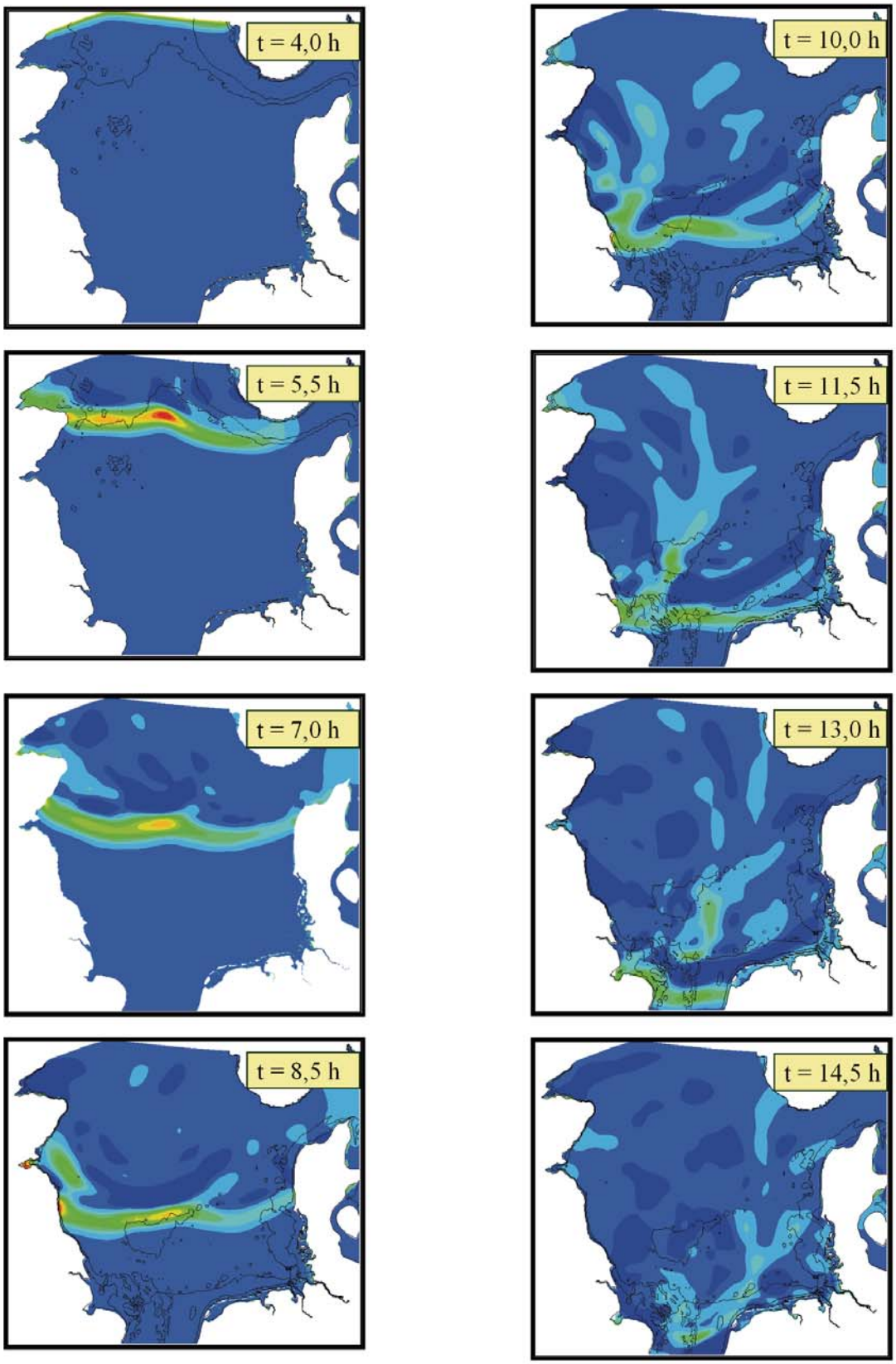

Fig. 10: Propagation of a tsunami (H = 6 m, geometrical wave input signal, coarse grid) in the North Sea

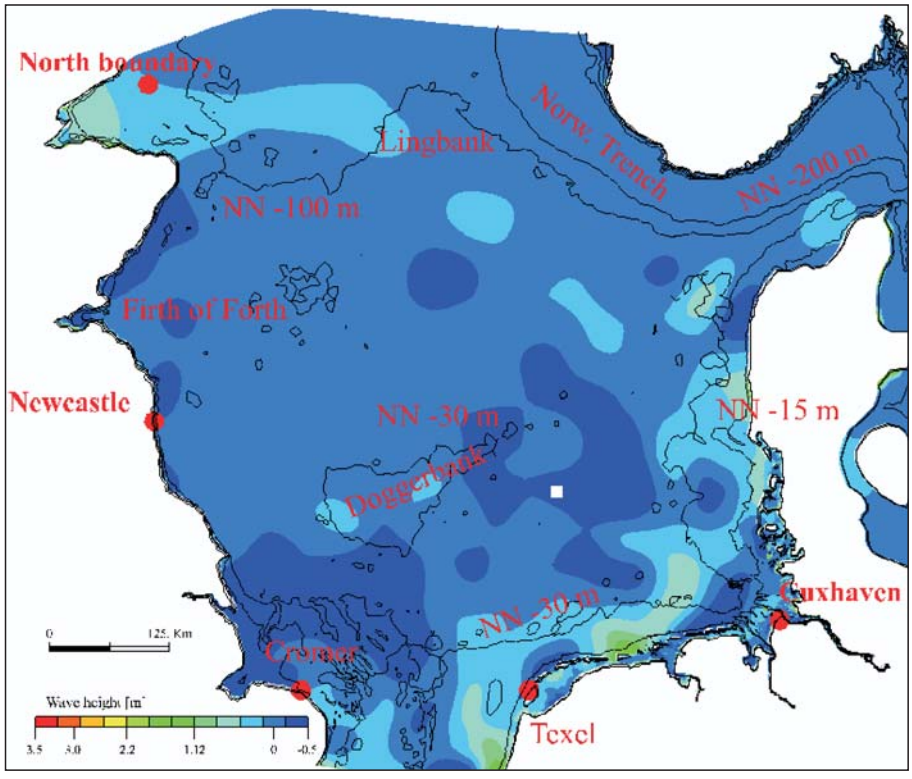

Fig. 11: Wave disturbance in the North Sea after passage of a tsunami

An analysis of wave heights at locations indicated in Fig. 11 along the English coast shows a double maximum at Newcastle, which occurs about 5 hours after arrival of the tsunami in the North Sea. The double peaks arrive at the English Channel (Cromer) and at the Dutch coast (Texel) with a time lag of about 2 to 3 hours. The time difference between the double peaks increases in the German Bight to up to 6 hours at Cuxhaven (Fig. 12).

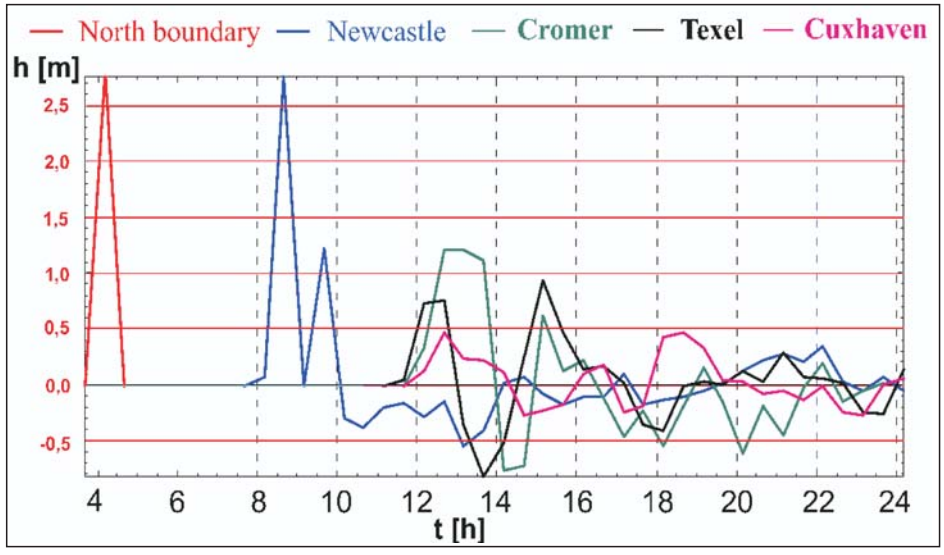

Fig. 12: Deformation of a tsunami wave in the North Sea (H = 3 m at Northern boundary)

The wave height of the tsunami decreases in the German Bight significantly to about 1/6 of the wave height at the Northern boundary of the North Sea. Fig. 13 illustrates the damping of the double peaks at the island of Helgoland, and for the onshore locations Emden, Wilhelmshaven, Bremerhaven and Cuxhaven at the entrances of the German estuaries. In this case, the initial tsunami wave height of H = 6 m is reduced to values of H ≈ 1 m along the German coast with maximum values at Emden, which are due to the generally larger wave heights observed at the Dutch coast as shown in Fig. 11.

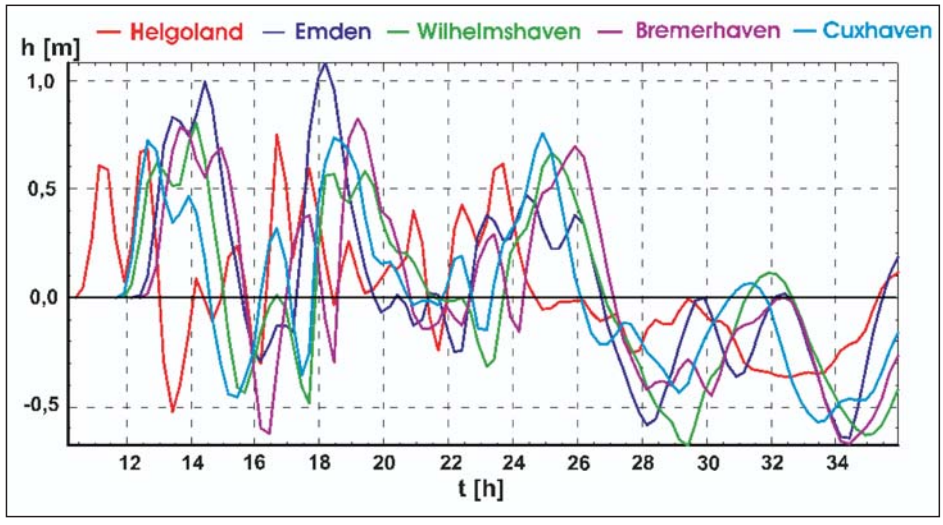

Fig. 13: Tsunami wave height at locations in the German Bight (H = 6 m at Northern boundary)

An analysis of wave heights on transects along the German barrier islands in the North Sea shows that the distribution of the maxima and minima is very non-uniform. The computed wave heights along the transect Borkum–Helgoland–Sylt are plotted in Fig. 14. During the passage time of the tsunami wave the hourly profiles document regions with quite different amplitudes in variation of wave heights.

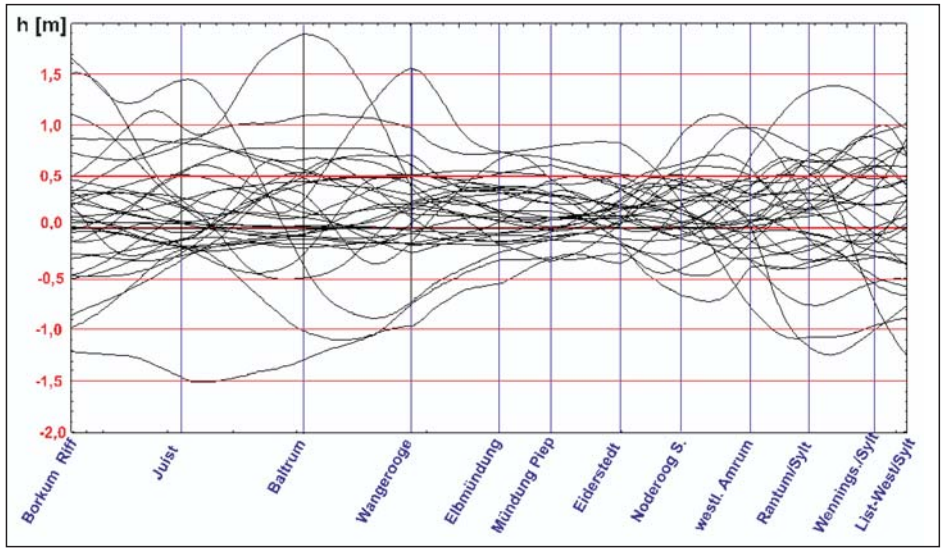

Fig. 14: Wave heights along the German coast (H = 6 m at Northern boundary)

The lowest wave heights have been found between the Elbe estuary and Eiderstedt while the highest ones occur along the East Frisian Islands in keeping with Fig. 11 and also in the neighbourhood of the island of Sylt.

The tsunami propagates in an estuary like a tidal bore up to the tidal limit without a significant decrease of the wave heights. Several individual waves are generated in the estuaries by reflection with amplitudes in the order of the first wave. Three maxima have been found at Zollenspieker (Fig. 15).

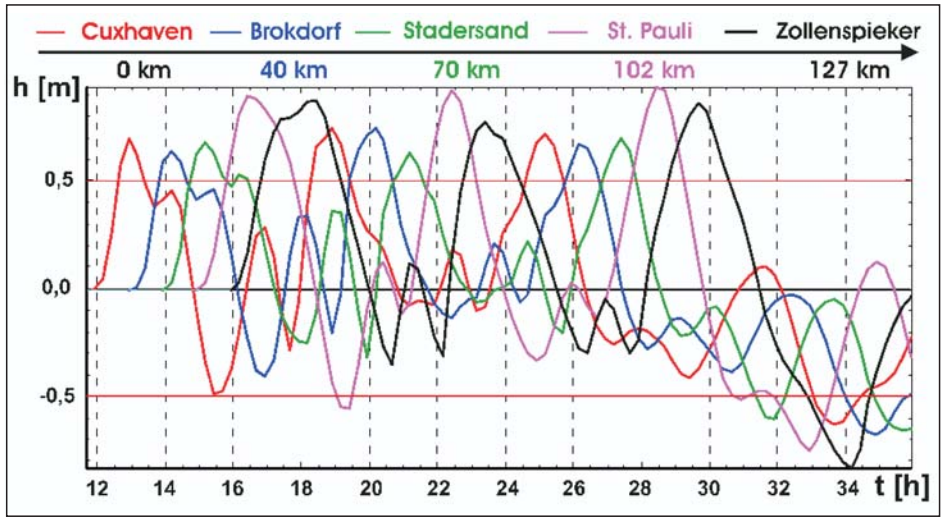

Fig. 15: Tsunami propagation in the Elbe estuary (H = 6 m at Northern boundary)

Water level variations of up to 2 metres within 1 to 2 hours result in rapid filling and draining processes of the wadden areas and the intertidal bays causing high local current velocities (Fig. 16). Computed velocities of approx. 1.0 m/s are in the same order of magnitude as observed during the Sumatra tsunami (SCHEFFER, 2005).

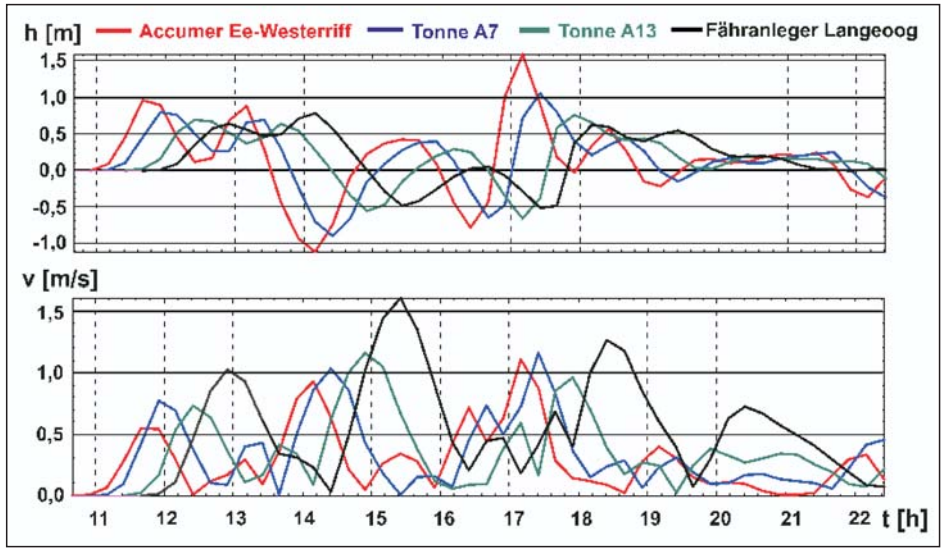

Fig. 16: Current velocities and water level variations (H = 6 m at Northern boundary)

4.2 Tsunami Propagation with Tidal Influence

To investigate the influence of tidal motion on a tsunami wave propagating towards the German Bight, three model runs were set up:

1. Only tidal motion (tide only),
2. tsunami wave input added to the tidal motion (tide + tsunami) and
3. only tsunami wave (tsunami only).

H = 3 m was chosen as forcing tsunami wave height for a geometric wave.

The difference between run 2 and 1 results in time series of water level variations due to a tsunami superposed on a tidal wave (tide + tsunami – tide), where the propagation of the tsunami wave is influenced by the tidal motion. In relation to run 3 the effect of the tidal water levels and the currents can be evaluated.

It is obvious from Fig. 17 that the tsunami wave is deformed at low tide due to the tidal current propagating against the tsunami. Variations of the tsunami wave at high tide are small compared to the variations at low tide.

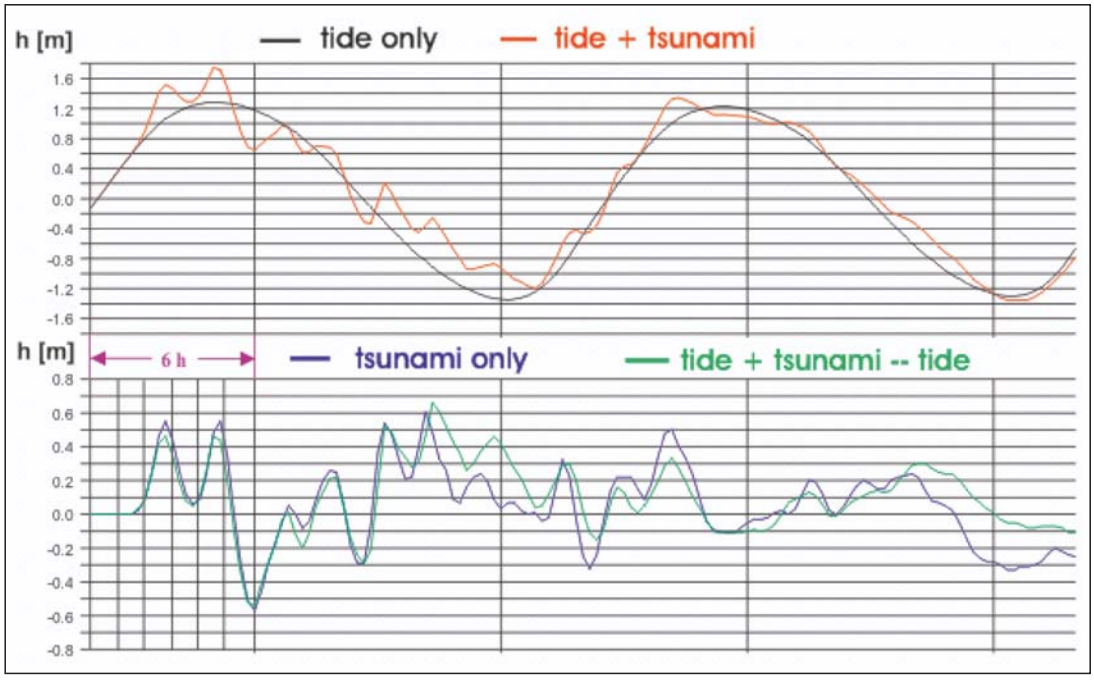

Fig. 17: Influence of tide on tsunami propagation, gauge Helgoland (H = 3 m at Northern boundary)

4.3 Tsunami Propagation Simulated in Different Models

Three different modeling approaches outlined in section 3.3 were used to study the propagation of a tsunami wave in the North Sea. The results given in Fig. 18 are comparable. The phase is quite similar while the maximum height and the length of the tsunami are slightly different. The differences are generated partly at the boundary because of the different forcing algorithms. These results are in keeping with a recently published study regarding the development of tsunami waves in the North Sea by BORK (2007).

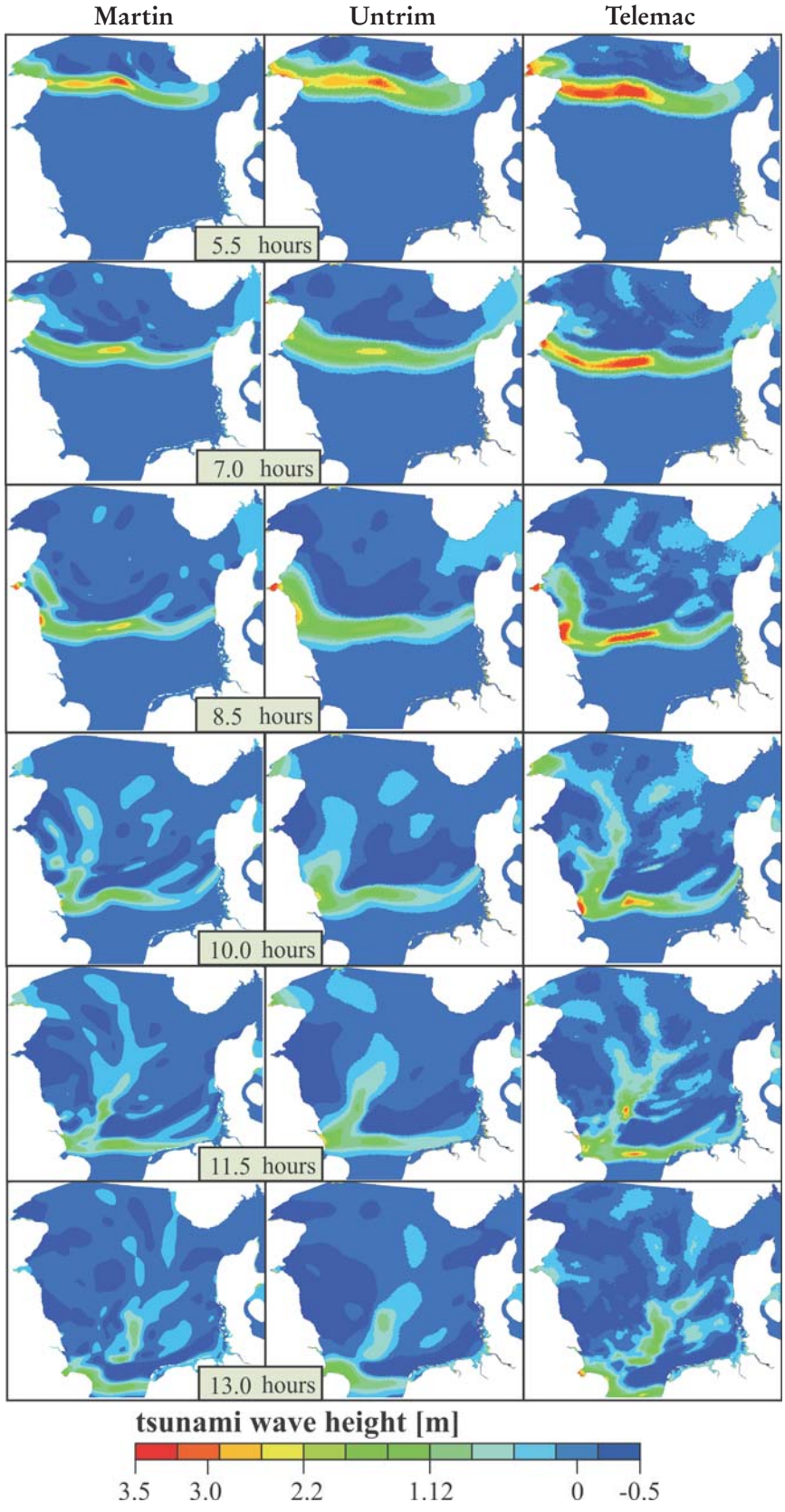

Fig. 18: Tsunami propagation in three different models

5. Summary and Conclusions

The shape and bathymetry of the North Sea and the German Bight are a good protection against tsunami waves. However, the Dutch coast and the British Island are not as well protected as the German coast. An incoming tsunami wave at the Northern boundary of the North Sea is transformed by shoaling, refraction, reflection and energy losses mainly by wave breaking. The amplitudes of a tsunami wave at the German North Sea coast can be compared to the water level elevations during a storm surge event. The governing processes are, of course, different.

6. References

BORK, I.; DICK, S.; KLEINE, E. and MÜLLER-NAVARRA, S.: Tsunami – a study regarding the North Sea coast. Berichte des Bundesamtes für Seeschifffahrt und Hydrographie, Nr. 41/2007.

CARRIER, G. F. and GREENSPAN, H. P.: Water Waves of Finite Amplitude on a Sloping Beach. J. Fluid Mech., 95, pp. 401–414, 1958.

CASULLI, V. and WALTERS, R. A.: An Unstructured Grid, Three-dimensional Model Based on the Shallow Water Equations. International Journal for Numerical Methods in Fluids; Vol. 32, No. 3, pp. 331–348, 2000.

DEAN, R. G. and DALRYMPLE, R. A.: Water Wave Mechanics for Engineers and Scientists. World Scientific. Advanced Series on Ocean Engineering. Vol. 2, 1991.

DEPARTMENT OF METEOROLOGY, MALDIVES: Time Series of Water Level at Male. 2004. http://ilikai.soest.hawaii.edu/uhslc/iot1d/male1.html

DIETRICH, G.; KALLE, K.; KRAUSS, W. and SIEDLER, G.: Allgemeine Meereskunde – Eine Einführung in die Ozeanographie. Bornträger, Stuttgart, 1975.

HERVOUET, J.-M.: Hydrodynamics of Free Surface Flows. Modelling with the finite element method. Wiley, Chichester, p 341, 2007.

KORTEWEG, D. J. and DEVRIES, G.: On the Change of Form of Long Waves Advancing in Rectangular Channel, and on a New Type of Long Stationary Waves. Philos. Mag. 5th Ser., Vol. 39, pp. 422–433, 1895.

LI, Y. and RAICHLEN, F.: Solitary Wave Run-up on Plane Slopes. Journal of Waterway, Port, Coastal, and Ocean Engineering. Vol. 127, No. 1, pp. 33–44, 2001.

LIN, P.; CHANG, K. and LIU, P.: Runup and Rundown of Solitary Waves on Sloping Beaches. Journal of Waterway, Port, Coastal and Ocean Engineering. Vol. 125, No. 5, pp. 247–255, 1999.

MILBRADT, P.: Martin Strömungsmodell. 2000. http://www.bauinf.uni-hannover.de/~milbradt/Martin/Current/current.html

NOAA MAGAZINE: NOAA scientists able to measure tsunami height from space, 2005. http://www.noaanews.noaa.gov/stories2005/s2365.htm

PLÜß, A. D. and SCHÜTTRUMPF, H.: Comparison of Numerical Tidal Models for Practical Applications. In JM Smith (ed) Proc. 29th Intl. Conf. Coastal Engineering. World Scientific, New Jersey, pp. 1199–1211, 2004.

PLÜß, A.: Das Nordseemodell der BAW zur Simulation der Tide in der Deutschen Bucht. Die Küste, H. 76, pp. 83–127, 2003.

SCHEFFER, H. J.: Tsunami-Schäden auf Sri-Lanka. HANSA. 142. Jahrgang. Nr. 3, pp. 56–57, 2005.

SPIELVOGEL, L. Q.: Single Wave Run-up on Sloping Beaches. Journal of Fluid Mechanics. No. 74, pp. 685–694, 1976.

STRYBNY, J.: Dissertation. Ein phasenauflösendes Seegangsmodell zur Ermittlung von Bemessungsparametern für Küstenstrukturen. Dissertation, Institut für Strömungsmechanik, Universität Hannover, Bericht Nr. 69, 2004.

SYNOLAKIS, C. E.: The Run-up of Solitary Waves. Journal of Fluid Mechanics. Vol. 185, pp. 523–545, 1987.

SYNOLAKIS, C. E. and SKJELBREIA, J. E.: Evolution of Maximum Amplitude of Solitary Waves on Plane Beaches. Journal of Waterway, Port, Coastal, and Ocean Engineering, Vol. 119, No. 3, pp. 323–342, 1993.

TUCK, E. O. and HWANG, L. S.: Long Wave Generation on a Sloping Beach. J. Fluid Mech., 51, pp. 449–461, 1972.